



Cite this: *Dalton Trans.*, 2016, **45**, 6032

Novel B(Ar')₂(Ar'') hetero-tri(aryl)boranes: a systematic study of Lewis acidity†

Robin J. Blagg,* Trevor R. Simmons, Georgina R. Hatton,‡ James M. Courtney, Elliot L. Bennett, Elliot J. Lawrence and Gregory G. Wildgoose*

A series of homo- and hetero-tri(aryl)boranes incorporating pentafluorophenyl, 3,5-bis(trifluoromethyl)phenyl, and pentachlorophenyl groups, four of which are novel species, have been studied as the acidic component of frustrated Lewis pairs for the heterolytic cleavage of H₂. Under mild conditions eight of these will cleave H₂; the rate of cleavage depending on both the electrophilicity of the borane and the steric bulk around the boron atom. Electrochemical studies allow comparisons of the electrophilicity with spectroscopic measurements of Lewis acidity for different series of boranes. Discrepancies in the correlation between these two types of measurements, combined with structural characterisation of each borane, reveal that the twist of the aryl rings with respect to the boron-centred trigonal plane is significant from both a steric and electronic perspective, and is an important consideration in the design of tri(aryl)boranes as Lewis acids.

Received 2nd October 2015,
Accepted 28th October 2015

DOI: 10.1039/c5dt03854e

www.rsc.org/dalton

Introduction

Since the initial report by Welch and Stephan¹ there has been rapid growth in studies of frustrated Lewis pairs (FLPs).^{2–7} In the archetypal system the Lewis acid, B(C₆F₅)₃, and Lewis base, P(^tBu)₃, are combined and are restricted from forming a classical Lewis acid–base adduct due to their steric bulk. Upon the addition of H₂, however, this FLP heterolytically cleaves H₂ to give protic and hydridic products.

FLPs in conjunction with H₂ have found applications as mediators or catalysts for metal-free hydrogenation of numerous functional groups including; aldehydes and ketones,^{8–10} N-heterocyclic aromatics,¹¹ imines and nitriles,¹² and silyl enol ethers.¹³ FLPs have also been shown to react with other small molecules such as oxides of carbon,^{14–16} nitrogen,¹⁷ and sulfur,¹⁸ along with alkenes and alkynes.^{19,20}

School of Chemistry, University of East Anglia, Norwich, NR4 7TJ, UK.

E-mail: g.wildgoose@uea.ac.uk, r.blagg@uea.ac.uk

† Electronic supplementary information (ESI) available: Characterisation data for the impurity B{3,5-(CF₃)₂C₆H₃}₂(OH), characterisation data for the intermediate B{3,5-(CF₃)₂C₆H₃}₂(OMe)₂; further details on the X-ray crystallographic studies of **5**, **6**; further details on the DFT calculations; reproductions of the previously published cyclic voltammograms of **1** and **4**, cyclic voltammograms of B{3,5-(CF₃)₂C₆H₃}₂(OH); further details for the NMR characterisation of the Et₃PO adducts of **1–9**, and correlation plots between the four different potential measures of Lewis acidity; further details for the H₂ cleavage by 1–9/P(^tBu)₃, including the time resolved ¹H and ¹¹B NMR spectra monitoring the reactions. CCDC 1418145 (**5**) and 1418144 (**6**). For ESI and crystallographic data in CIF or other electronic format see DOI: 10.1039/c5dt03854e

‡ Current address: School of Chemistry, The University of Manchester, Oxford Road, Manchester, M13 9PL, UK.

Tris(pentafluorophenyl)borane, B(C₆F₅)₃, is the most commonly used Lewis acidic component of FLPs; although other electrophilic boranes have been used in FLPs (or suggested for use in FLPs), such as other halogenated tri(aryl)boranes^{9,15,21–23} including the stepwise-substitution series B(C₆Cl₅)_n(C₆F₅)_{3–n} (*n* = 1–3),^{24,25} and B{2,4,6-(CH₃)₃C₆H₂}_n(C₆F₅)_{3–n} (*n* = 1–3),²⁶ and borenium cations (commonly stabilised by N-heterocycle carbenes).^{27,28} Not all Lewis acids used in FLPs have been boron based, with other examples including; Ingleson and co-workers' carbon-based, water tolerant *N*-methylacredinium salts,²⁹ tri(aryl)aluminium analogues of classical boron based species,³⁰ both phosphorus(III) and phosphorus(V)-based species,³¹ and silicon based species.^{32,33}

We have previously introduced the concept of “combined electrochemical-frustrated Lewis pairs”,^{28,34–37} where the heterolytic cleavage of H₂ by an FLP is coupled with *in situ* electrochemical oxidation of the resulting Lewis acid-hydride, liberating two electrons, a proton, and regenerating the parent Lewis acid. Hence, we have shown these systems to be electrocatalytic for the oxidation of H₂ to yield two protons and two-electrons overall – a key process for many hydrogen-based energy technologies.

To further develop our “combined electrochemical-frustrated Lewis pair” concept, we sought to expand the range of tri(aryl)borane Lewis acids allowing us to probe the effects of further controlled modification of the boranes. Our existing studies having focused on the archetypal B(C₆F₅)₃,^{34,35} its perchlorinated analogue,³⁶ three isomers of B{C₆H₃(CF₃)₂}₃,³⁷ along with the borenium cation [(^tPrN)₂H₂C₃BC₉H₁₄]⁺.²⁸ The stepwise substitution of the aryl rings would result in a range



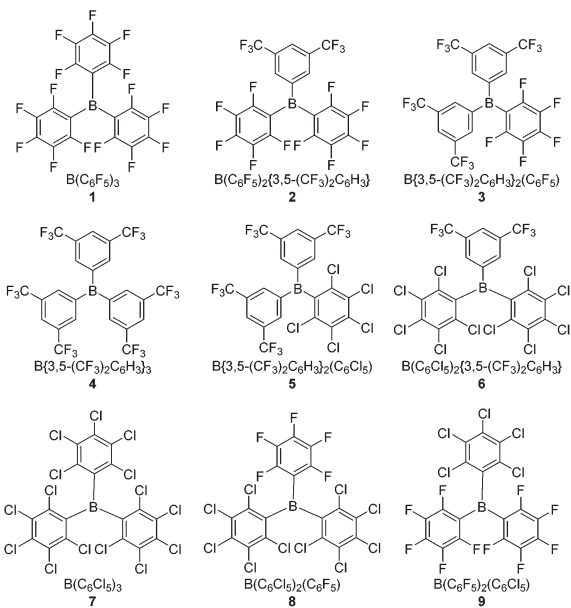


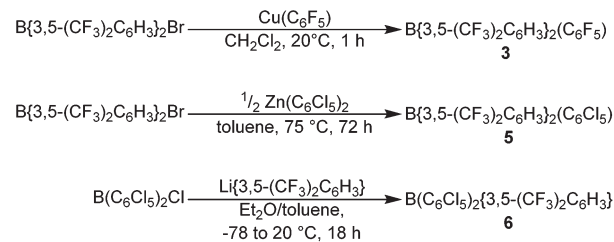
Fig. 1 Homo- and hetero-tri(aryl)boranes, $B(Ar')_2(Ar'')/BArHal_x$.

of 2:1 hetero-tri(aryl)boranes, in addition to the existing homo-tri(aryl)boranes. It was envisaged that by altering the electronic and steric nature of successive aryl groups, that the Lewis acidic boranes would exhibit varying properties (*e.g.* reactivates towards H_2 activation, chemical tolerances, redox properties). Such a systematic study could also allow for insights into the chemical origin of these properties and provide further information toward a predictive model for reactivities of tri(aryl)boranes.

Herein we report studies of four novel hetero-tri(aryl)boranes 2, 3, 5 and 6, incorporating combinations of the pentafluorophenyl (C_6F_5 , Ar^{F5}), 3,5-bis(trifluoromethyl)phenyl $\{3,5-(CF_3)_2C_6H_3$, $Ar^{F6}\}$, and pentachlorophenyl (C_6Cl_5 , Ar^{Cl5}) halogenated-aryl rings; together with further studies of the previously reported²⁴ tris(pentachlorophenyl)borane, 7, and the hetero-(pentachlorophenyl)(pentafluorophenyl)boranes 8 and 9. Comparing these with the archetypal Lewis acidic borane $B(C_6F_5)_3$, 1, and $B\{3,5-(CF_3)_2C_6H_3\}_3$, 4, allows for a comprehensive study of the effects of stepwise substitution of the aryl rings (Fig. 1). Both electrochemical and conventional NMR methodologies are employed to quantify the Lewis acidity/electrophilicity of the boranes, and the results of these methodologies compared. Finally, their potential to act as the Lewis acidic component of an FLP {in combination with the Lewis base tri-*tert*-butylphosphine (tBu_3P)} for the heterolytic cleavage of H_2 under mild conditions is studied.

Results & discussion

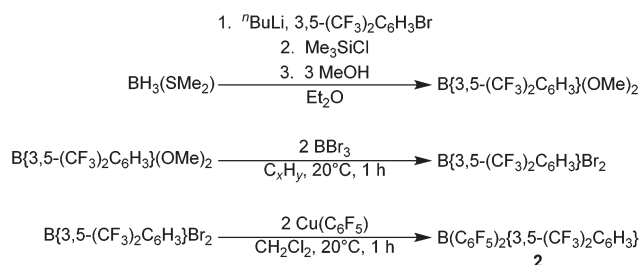
The novel hetero-tri(aryl)boranes 3, 5 and 6, were all synthesised by broadly similar methods (Scheme 1), involving the reaction of a bis(aryl)haloborane with a suitable metal-aryl



Scheme 1 Synthetic routes for the synthesis of 3, 5 and 6.

transfer agent. Reaction of $B\{3,5-(CF_3)_2C_6H_3\}_2Br$ with $Cu(C_6F_5)$ in CH_2Cl_2 at room temperature, or $Zn(C_6Cl_5)_2$ in toluene at $+75^\circ C$, led to synthesis of 3 and 5 respectively. In certain cases however, the impurity $B\{3,5-(CF_3)_2C_6H_3\}_2(OH)$ was obtained (characterisation data in ESI[†]), due to reaction of the bis(aryl) bromoborane precursor with trace water or hydroxide, fortunately 3 and 5 can be isolated by sublimation or recrystallization, respectively. 6 is synthesised by the reaction of a toluene solution of $B(C_6Cl_5)_2Cl$ with *in situ* generated $Li\{3,5-(CF_3)_2C_6H_3\}$ in Et_2O solution at $-78^\circ C$ followed by slow warming to room temperature.

Applying this methodology for the synthesis of 2, by reaction of $B(C_6F_5)_2X$ ($X = F, Cl$) with $M\{3,5-(CF_3)_2C_6H_3\}$ ($M = Li, Cu$) under various conditions, we were unable to obtain 2 as anything other than a minor component in a mixture of species. Therefore an alternative synthetic route was developed (Scheme 2). Following on from the publication by Samigullin *et al.*³⁸ of a high yielding stepwise route for the synthesis of $B\{3,5-(CF_3)_2C_6H_3\}_2Br$, we were able to successfully adapt their methodology for the synthesis of $B\{3,5-(CF_3)_2C_6H_3\}_2Br_2$. This required the generation of $Li\{3,5-(CF_3)_2C_6H_3\}$ at $-78^\circ C$, and its reaction in Et_2O with $BH_3 \cdot SME_2$ to give $[Li(OEt)_2]_n[LiH_3B\{3,5-(CF_3)_2C_6H_3\}]$. Hydride abstraction using one equivalent Me_3SiCl gave $BH_2\{3,5-(CF_3)_2C_6H_3\}$, and reaction with excess methanol converts the bis-hydride to the bis-methoxide $B\{3,5-(CF_3)_2C_6H_3\}(OMe)_2$ (characterisation data in ESI[†]). Conversion of the bis-methoxide to the bis-bromide was readily achieved by reaction with excess BBr_3 , leading to the isolation of highly reactive $B\{3,5-(CF_3)_2C_6H_3\}_2Br_2$ as a pale yellow oil. Further reaction with two equivalents of $Cu(C_6F_5)$ in CH_2Cl_2 , results in the rapid generation of 2, which may be purified *via* sublimation.



Scheme 2 Synthetic route for the synthesis of 2.



The syntheses of 7–9 have previously been reported by Ashley *et al.*,²⁴ however we found a number of minor changes to the published methodologies were necessary to synthesise these compounds. For the lithium–halogen exchange of C₆Cl₆ and ⁿBuLi to generate LiC₆Cl₅, we found control of temperature was critical with *any* temperature increase above –78 °C leading to an unacceptably high generation of decomposition products. Additionally we found that due to the sparing solubility of C₆Cl₆ in Et₂O using as large a volume of solvent as practical was advantageous for initial lithiation. Of equal importance was the addition of an anti-solvent (*n*-pentane) in approximately a 3:2 ratio to precipitate out the aryl-lithium compound, so as to avoid the risk of undesirable Et₂O cleavage products, as previously reported by Ashley *et al.*²⁴ These modifications allowed for the synthesis of 7 (by reaction of three equivalents of LiC₆Cl₅ with BCl₃), and B(C₆Cl₅)₂Cl (by reaction of two equivalents of LiC₆Cl₅ with BCl₃, precursor for 8), and B(C₆Cl₅)Br₂ (by reaction of half an equivalent of Zn(C₆Cl₅)₂ with BBr₃, precursor for 9), to be readily achievable. Compound 9 was obtained by reaction of B(C₆Cl₅)Br₂ with two equivalents of Cu(C₆F₅) and purification by sublimation as previously reported. Rather than using the published synthesis of 8, by reaction of B(C₆Cl₅)₂Cl with Cu(C₆F₅) in toluene at +80 °C, we successfully synthesised 8 by reaction of B(C₆Cl₅)₂Cl with freshly generated LiC₆F₅ in a toluene solution at –78 °C followed by slow warming to room temperature, and extraction into *n*-hexane.

Structural studies

X-ray crystal structures were obtained from single crystals of 5 (grown by slow diffusion of a saturated CH₂Cl₂ solution into *n*-hexane at –25 °C), and 6 (grown from a saturated *n*-hexane solution at –25 °C) (Fig. 2a and b and S1a and b,† Table 5).

We have been unable to grow single crystals of 1–3, so instead, geometry optimised structures have been calculated computationally {at the B3LYP/6-311+G(d,p) level of theory, see ESI† for further details} (we previously reported the calculated structure of 1³⁴) (Fig. S2a–c†); calculated structures of 4–8 do not show significant differences when compared to their X-ray crystal structures, thereby validating this approach. {9 is an exception, due to the two Ar^{F5} rings having significantly different twist-angles (assumed to be due to crystal packing effects) in the crystal structure, a feature that is not reproduced in the calculated structure.}

The crystallographic and calculated structures of 1–3, 5 and 6, along with the previously published crystal structures of 4³⁹ and 7–9,²⁴ all show similar features: a trigonal-planar boron centre and the three aryl rings twisted with respect to the BC₃ plane, leading to a propeller type conformation, thereby minimising steric interactions between the aryl rings. The *ortho*-substituents would dominate such steric interactions leading to the smallest (13–36°) twist occurring for Ar^{F6} rings (*ortho*-H) the largest (56–80°) for the Ar^{Cl5} rings (*ortho*-Cl) with the Ar^{F5} rings (*ortho*-F) in the middle (22–52°), as shown in Table 1.

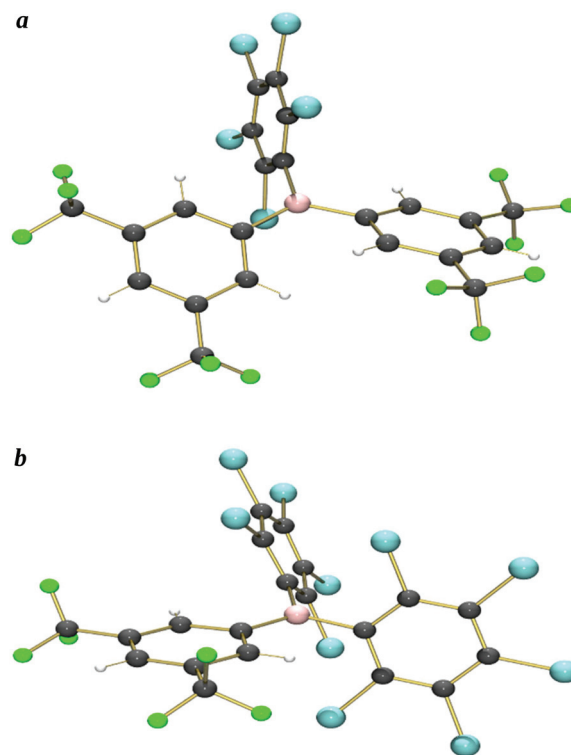


Fig. 2 (a) X-ray crystallographic structure of B{3,5-(CF₃)₂C₆H₃}₂(C₆Cl₅) 5. (b) X-ray crystallographic structure of B(C₆Cl₅)₂{3,5-(CF₃)₂C₆H₃} 6 (minor component of crystallographic disorder removed for clarity).

Table 1 Mean (standard deviation) twist-angles of aryl ring(s) from BC₃ plane

	Ar ^{F5}	Ar ^{F6}	Ar ^{Cl5}
B(C ₆ F ₅) ₃ 1 ³⁴	37.0° ^a	—	—
B(C ₆ F ₅) ₂ {3,5-(CF ₃) ₂ C ₆ H ₃ } 2	51.7° ^a	25.1° ^a	—
B{3,5-(CF ₃) ₂ C ₆ H ₃ } ₂ (C ₆ F ₅) 3	51.1° ^a	30.8° ^a	—
B{3,5-(CF ₃) ₂ C ₆ H ₃ } ₃ 4 ³⁹	—	36(2)°	—
B{3,5-(CF ₃) ₂ C ₆ H ₃ } ₂ (C ₆ Cl ₅) 5	—	26(1)°	79.7° ^b
B(C ₆ Cl ₅) ₂ {3,5-(CF ₃) ₂ C ₆ H ₃ } 6	—	13(0)°	62(2)°
B(C ₆ Cl ₅) ₃ 7 ²⁴	—	—	56(3)°
B(C ₆ Cl ₅) ₂ (C ₆ F ₅) 8 ²⁴	22(1)°	—	59(3)°
B(C ₆ F ₅) ₂ (C ₆ Cl ₅) 9 ²⁴	38(16)° ^c	—	70(1)°

^a Crystal structure not known, angles from optimised {B3LYP/6-311+G(d,p)} structure. ^b Crystallographic symmetry leads to only one unique twist-angle. ^c Each aryl ring has significantly different twist-angle: 52(1), 24(2)°.

As the twist-angles of the aryl rings vary, changes in the electronic interactions of the ring and its substituents with the boron centre can be implied. Firstly, large twist-angles orientate the rings such that their *ortho*-substituents are above/below the boron centred trigonal plane, creating the potential for through-space donation of any lone pair electron density on the *ortho*-substituents into the formally vacant boron 2p_z orbital, as we have shown to occur for the *ortho*-CF₃ substituents of the 2,4- and 2,5-isomers of 4.³⁷ Secondly, as the twist-



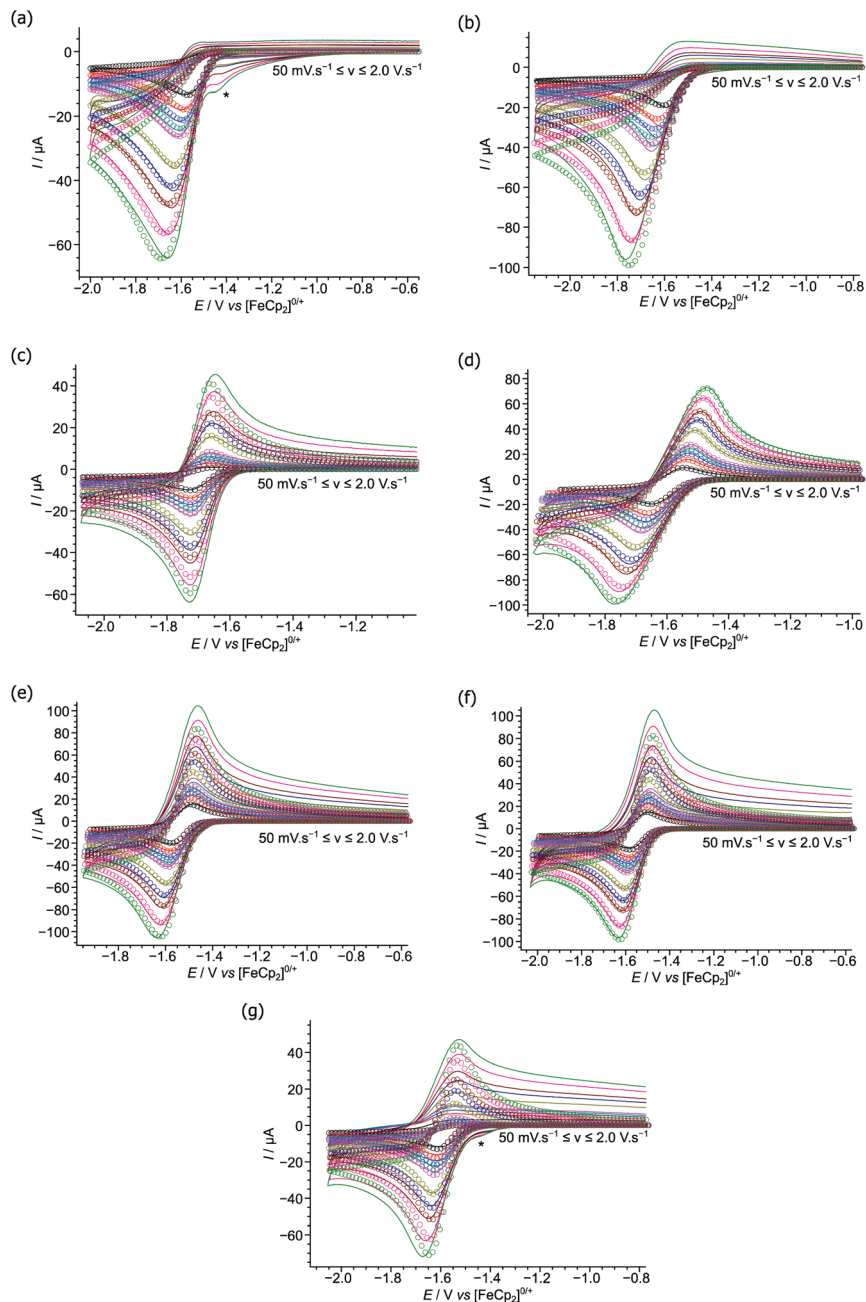


Fig. 3 Experimental (line) and simulated (open circles) cyclic voltammograms for the reduction of: (a) $B(C_6F_5)_2\{3,5-(CF_3)_2C_6H_3\}$ **2**; (b) $B\{3,5-(CF_3)_2C_6H_3\}_2(C_6F_5)$ **3**; (c) $B\{3,5-(CF_3)_2C_6H_3\}_2(C_6Cl_5)$ **5**; (d) $B(C_6Cl_5)_2\{3,5-(CF_3)_2C_6H_3\}$ **6**; (e) $B(C_6Cl_5)_3$ **7**; (f) $B(C_6Cl_5)_2(C_6F_5)$ **8**; (g) $B(C_6F_5)_2(C_6Cl_5)$ **9**. Shoulders (*) visible at the higher scan rates due to trace impurity in the solvent/electrolyte.

angle decreases, symmetry considerations imply an increase in overlap between the boron $2p_z$ orbital and the filled ($2p_z$ derived) π orbitals of the aromatic ring (while electronic effects *via* σ -bonding between the boron and aryl rings should be independent of the twist-angle of the aryl rings). In both these cases, donation of electron density into the boron $2p_z$ orbital would be expected to attenuate the borane's Lewis acidity, influencing both its observed electrochemical properties and reactivity.

Electrochemical studies

Cyclic voltammograms were obtained at varying scan rates for **2**, **3**, **5**–**9** (Fig. 3), at a glassy carbon electrode, in the weakly-coordinating solvent CH_2Cl_2 using $[^nBu_4N][B(C_6F_5)_4]$ as the added electrolyte, and compared with those previously reported by this group under the same conditions for **1** and **4** (reproduced in Fig. S3a and b†).³⁷ Note that whilst electrochemical studies of **7**–**9** have been previously reported,²⁴ we



have repeated the measurements herein to ensure they are comparable with our other results. This is especially true considering our use of the weakly-coordinating anion $[\text{B}(\text{C}_6\text{F}_5)_4]^-$ in the electrolyte together with a glassy carbon *macro*-electrode, in contrast to the previously reported voltammograms using an electrolyte containing the potentially non-innocent $[\text{BF}_4]^-$ anion and a platinum *micro*-electrode.

There are three general behaviours observed in the cyclic voltammograms recorded for boranes 1–9. The first, for 2–4, showing completely irreversible reductions at all scan rates studied (50 mV s^{-1} to 2.0 V s^{-1}), indicating very rapid reaction/decomposition of the radical-anion intermediate generated upon reduction of the parent borane.³⁴ The second, for 1, 5 & 9, appear irreversible at slower scan rates yet as the scan rates increase appear *quasi*-reversible as the kinetics of the homogeneous follow-on chemical decomposition step are outrun on the voltammetric timescale. Finally, 6–8, appear *quasi*-reversible over the entire range of scan rates.

To quantify the observed redox behaviours we performed digital simulations of the experimental voltammetric data, modelling the redox processes using an EC-mechanism³⁴ (*i.e.* a reversible, heterogeneous electron transfer step followed by an irreversible, homogeneous chemical step generating electro-inactive products – other postulated mechanisms produce a poor fit to the data). These digital simulations allowed us to extract pertinent mechanistic parameters such as the formal redox potentials and charge transfer coefficients (E° and α respectively) and kinetic parameters for the electron transfer (k^0) and follow-on chemical step (k_f) as shown in Table 2 (together with our previously reported parameters for 1 and 4).

These formal redox potentials are a measure of the electrophilicity of the LUMO (formally the vacant boron $2p_z$ orbital), and one might expect them to correlate to the Lewis acidity of the free borane; the more negative the E° value, the less electrophilic the boron. When considering only the homo-tri(aryl) boranes 1, 4 & 7, the observed redox potential imply that the net electron withdrawing effect of the aryl rings increases

(thereby making the boron more electrophilic) in the order $\text{Ar}^{\text{F6}} < \text{Ar}^{\text{Cl5}} \approx \text{Ar}^{\text{F5}}$. This is contrary to the description of Ar^{Cl5} as more electron withdrawing than Ar^{F5} (due to back-donation of the filled fluorine $2p$ orbitals into the aromatic π^* orbitals counteracting its high electronegativity, this effect is much reduced for chlorine due to the poorer overlap of $3p$ orbitals with the aromatic π orbitals; as shown by Hammett parameters: $\sigma_{\text{paraCl}} = 0.227$, $\sigma_{\text{paraF}} = 0.062$).²⁴ We propose that this is due to through-space interaction between the *ortho*-Cl substituents with the boron centre in 7 ($\text{B}\cdots\text{Cl}$ *ca.* 3.1 Å), quenching the electrophilicity by donation of electron density from the chlorine lone pairs into the formally empty boron $2p_z$ orbital. The orientation {large twist-angle, 56(3)°, orientating *ortho*-Cl above/below the BC_3 trigonal-plane} and size of the chlorine $3p$ orbitals, make such interaction much more favourable than for 1; an effect which might also be expected to occur to a varying degree for all the other boranes incorporating Ar^{Cl5} substituents, 4, 5, 8 & 9.

Further discussion of the trends in E° is given below, but a linear trend can clearly be observed for the series 1–4: $\text{B}(\text{Ar}^{\text{F5}})_x(\text{Ar}^{\text{F6}})_y$ (the stepwise substitution of Ar^{F5} with Ar^{F6}). Similar experiments performed for the series $\text{B}\{2,4,6\text{-(CH}_3)_3\text{C}_6\text{H}_2\}_n(\text{C}_6\text{F}_5)_{3-n}$ ($n = 1\text{--}3$)²⁶ at a Pt disc in $\text{thf}/[\text{t}^n\text{Bu}_4\text{N}][\text{B}(\text{C}_6\text{F}_5)_4]$, displayed a pronounced linear change in $E_{1/2}$ varying by *ca.* 500 mV as each mesityl ring was substituted with a C_6F_5 ring.

Additionally, since the reversibility of the voltammograms is dependent on the stability of the radical-anion intermediate generated upon reduction of the parent borane, and as we have previously reported,^{34,37} it is assumed that the decomposition pathway proceeds *via* interaction of the radical-anion with the solvent, it may be implied that the slower the rate of decomposition (quantified by the rate constant k_f), the more steric shielding is present around the boron centre to stabilise the radical anion. Hence, the presence of Ar^{Cl5} ring(s) reduces k_f values by *up to* five orders of magnitude due to its high steric bulk (due to the *ortho*-Cl substituents and the associated high twist-angles), compared to the Ar^{F5} and Ar^{F6} rings alone.

Table 2 Simulation parameters for the one-electron reductions of $\text{B}(\text{Ar}')_2(\text{Ar}'')$

	$\text{BArHal}_x + e^- \rightleftharpoons \text{BArHal}_x^{\cdot-}$			$\text{BArHal}_x^{\cdot-} \Rightarrow \text{decomposition}$	$D(\text{BArHal}_x) = D(\text{BArHal}_x^{\cdot-})/\text{cm}^2 \text{ s}^{-1} \text{ }^a$
	E°/V vs. $[\text{FeCp}_2]^{0/+}$	α	$k^0/\text{cm s}^{-1}$	$k_f/\text{s}^{-1} \text{ }^b$	
$\text{B}(\text{C}_6\text{F}_5)_3$ 1 ³⁷	-1.52 ± 0.01	0.379	1.45×10^{-2}	9.2	0.85×10^{-5}
$\text{B}(\text{C}_6\text{F}_5)_2\{3,5\text{-(CF}_3)_2\text{C}_6\text{H}_3\}$ 2	-1.56 ± 0.01	0.300	8.45×10^{-3}	≥ 30	1.41×10^{-5}
$\text{B}\{3,5\text{-(CF}_3)_2\text{C}_6\text{H}_3\}_2(\text{C}_6\text{F}_5)$ 3	-1.57 ± 0.01	0.387	4.85×10^{-3}	≥ 25	1.18×10^{-5}
$\text{B}\{3,5\text{-(CF}_3)_2\text{C}_6\text{H}_3\}_3$ 4 ³⁷	-1.61 ± 0.01	0.419	4.56×10^{-3}	≥ 25	3.76×10^{-5}
$\text{B}\{3,5\text{-(CF}_3)_2\text{C}_6\text{H}_3\}_2(\text{C}_6\text{Cl}_5)$ 5	-1.70 ± 0.01	0.512	2.69×10^{-1}	0.36	2.54×10^{-5}
$\text{B}(\text{C}_6\text{Cl}_5)_2\{3,5\text{-(CF}_3)_2\text{C}_6\text{H}_3\}$ 6	-1.60 ± 0.01	0.415	1.14×10^{-2}	0.056	1.44×10^{-5}
$\text{B}(\text{C}_6\text{Cl}_5)_3$ 7	-1.54 ± 0.01	0.425	1.20×10^{-2}	$\leq 10^{-5}$	1.22×10^{-5}
$\text{B}(\text{C}_6\text{Cl}_5)_2(\text{C}_6\text{F}_5)$ 8	-1.54 ± 0.01	0.416	1.13×10^{-2}	$\leq 10^{-5}$	1.26×10^{-5}
$\text{B}(\text{C}_6\text{F}_5)_2(\text{C}_6\text{Cl}_5)$ 9	-1.58 ± 0.01	0.445	5.59×10^{-2}	0.88	1.68×10^{-5}

^a With exception of 7, all diffusion constants (D) obtained *via* ^1H and/or ^{19}F DOSY NMR spectroscopy. ^b k_f values are modelled as a *pseudo* first-order process.



Measurements of Lewis acidity

To-date common methods for the quantification of Lewis acidity have been based on spectroscopic techniques. One such technique, the “Gutmann–Beckett method”,^{40,41} involves adduct formation between the Lewis acid of interest and the Lewis base triethylphosphine-oxide (Et_3PO); and measurement of its ^{31}P chemical shift (commonly reported as the “acceptor number” – a normalised proxy for the observed chemical shift relative to that of free Et_3PO in hexane). With the rationale that increased Lewis acidity, results in de-shielding (and thereby an increase in chemical shift) of the bound phosphorus atom. A comprehensive study of Lewis acidic boron compounds was recently published by Sivaev and Bregadze,⁴² identifying a number of electronic effects which may influence the measurement of Lewis acidity by this method. As a measure of Lewis acid–base adduct formation the “Gutmann–Beckett method” is also somewhat limited by steric effects, and is blind to any associated electronic influences present in the trigonal planar parent borane that are no longer present in the tetrahedral adduct (such as through-space donation from *ortho*-substituents into the boron $2p_z$ orbital, as discussed above for the Ar^{Cl5} substituents). Considering that all our Lewis acids are boron based, we will also consider both the ^{11}B chemical shifts of the free boranes and their Et_3PO adducts as tools to measure Lewis acidity.

Spectral data for Et_3PO adducts of **1–6**, **8**, **9**, are detailed in Tables 3 and S1.† (As previously reported,²⁴ due to its steric bulk **7** will not form an adduct with Et_3PO , clearly identifying a limit on such methodology.)

Thereby we have three measures to quantify the Lewis acidity of different boranes: the ^{11}B chemical shift of the free borane, and the ^{31}P and ^{11}B chemical shifts of the Lewis acid–base adduct $\text{Et}_3\text{POB}(\text{Ar}^x)_2(\text{Ar}^y)$, together with the standard reduction potential (E°) of the free borane which measures the electrophilicity of the formally vacant $2p_z$ orbital of the boron (Table 2). Comparing the variation in these measures across the stepwise substitution of aryl rings in the boranes **1–9**

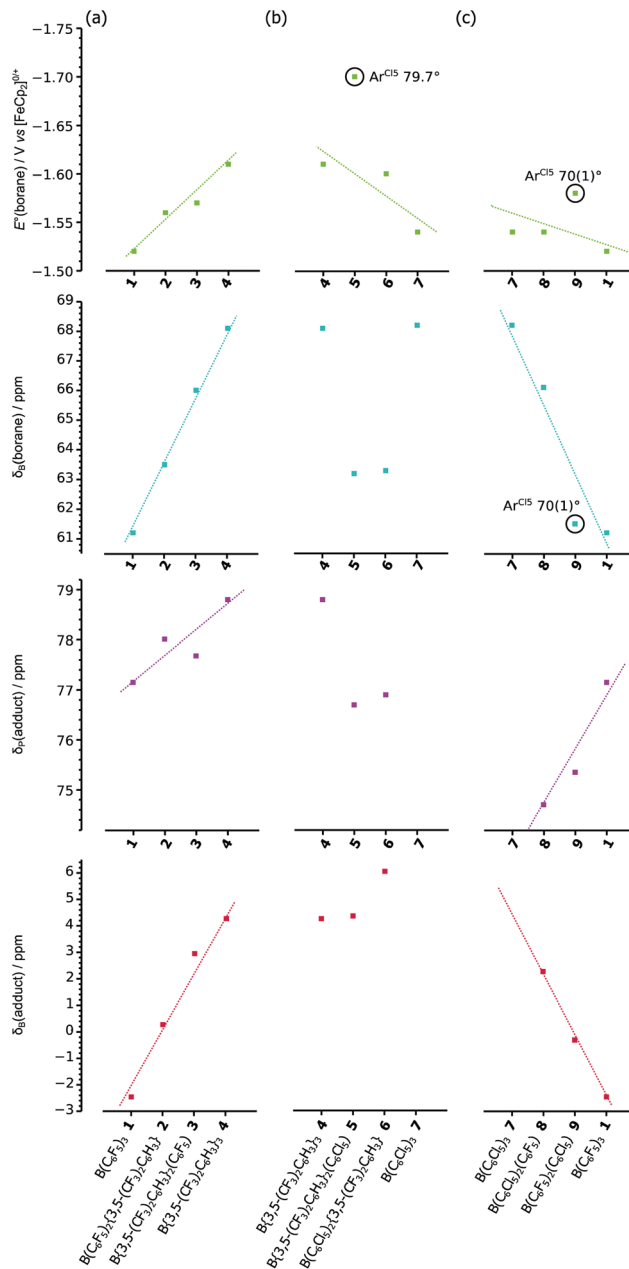


Fig. 4 Variation of $E^\circ(\text{borane})$, $\delta_{\text{B}}(\text{borane})$, $\delta_{\text{P}}(\text{adduct})$ and $\delta_{\text{B}}(\text{adduct})$; for (a) $\text{B}(\text{Ar}^{\text{F5}})_x(\text{Ar}^{\text{F6}})_y$ **1–4**, (b) $\text{B}(\text{Ar}^{\text{F6}})_y(\text{Ar}^{\text{Cl5}})_z$ **4–7**, and (c) $\text{B}(\text{Ar}^{\text{F5}})_x(\text{Ar}^{\text{Cl5}})_z$ **7–9** & **1**.

Table 3 Measurements of Lewis acidity: ^{31}P and ^{11}B NMR chemical shifts (in CD_2Cl_2) for the $\text{Et}_3\text{POB}(\text{Ar}^x)_2(\text{Ar}^y)$ adducts

	$\delta_{\text{P}}(\text{adduct})/\text{ppm}$	$\delta_{\text{B}}(\text{adduct})/\text{ppm}$
$\text{B}(\text{C}_6\text{F}_5)_3$ 1 ^a	+77.15	−2.46
$\text{B}(\text{C}_6\text{F}_5)_2\{3,5\text{-(CF}_3)_2\text{C}_6\text{H}_3\}$ 2	+78.01	+0.27
$\text{B}\{3,5\text{-(CF}_3)_2\text{C}_6\text{H}_3\}_2(\text{C}_6\text{F}_5)$ 3	+77.68	+2.95
$\text{B}\{3,5\text{-(CF}_3)_2\text{C}_6\text{H}_3\}_3$ 4	+78.80	+4.27
$\text{B}\{3,5\text{-(CF}_3)_2\text{C}_6\text{H}_3\}_2(\text{C}_6\text{Cl}_5)$ 5	+76.7 (br)	+4.37
$\text{B}(\text{C}_6\text{Cl}_5)_2\{3,5\text{-(CF}_3)_2\text{C}_6\text{H}_3\}$ 6	+76.9 (v.br)	+6.06
$\text{B}(\text{C}_6\text{Cl}_5)_3$ 7	No adduct formation	
$\text{B}(\text{C}_6\text{Cl}_5)_2(\text{C}_6\text{F}_5)$ 8 ^b	+74.70	+2.27
$\text{B}(\text{C}_6\text{F}_5)_2(\text{C}_6\text{Cl}_5)$ 9 ^c	+75.35	−0.31

All values herein have been re-measured by the authors, internally referenced to $\delta_{\text{P}}(\text{Et}_3\text{PO}) = +50.70$ ppm. ^a Previously reported in ref. 42 over the range $\delta_{\text{P}} +77.0$ to $+78.1$. ^b Previously reported in ref. 24 as $\delta_{\text{P}} +74.5$ and $\delta_{\text{B}} +0.3$. ^c Previously reported in ref. 24 as $\delta_{\text{P}} +75.8$ and $\delta_{\text{B}} -1.1$.

(Fig. 4), together with considering any correlation between all four measures (Fig. S5†), allows for general trends (and outliers) to be identified.

The series $\text{B}(\text{Ar}^{\text{F5}})_x(\text{Ar}^{\text{F6}})_y$, **1–4**, shows linear variations in all four measures across the series, with $-E^\circ$, $\delta_{\text{B}}(\text{borane})$, $\delta_{\text{P}}(\text{adduct})$ and $\delta_{\text{B}}(\text{adduct})$ all increasing as Ar^{F5} rings are substituted with Ar^{F6} rings.

The series $\text{B}(\text{Ar}^{\text{F6}})_y(\text{Ar}^{\text{Cl5}})_z$, **4–7**, shows clear trends only for $-E^\circ$ showing a general decrease as the Ar^{F6} rings are substituted with Ar^{Cl5} rings (with exception of **5**, which appears



higher than the trend otherwise implies). For $\delta_{\text{B}}(\text{borane})$, $\delta_{\text{P}}(\text{adduct})$ and $\delta_{\text{B}}(\text{adduct})$, any trends are relatively poor (further emphasised by the fact that an adduct of 7 cannot be formed).

Finally, the series $\text{B}(\text{Ar}^{\text{F5}})_x(\text{Ar}^{\text{Cl5}})_z$, 7–9, **1**, shows generally linear variations with $\delta_{\text{P}}(\text{adduct})$ increasing, while $-E^\circ$, $\delta_{\text{B}}(\text{borane})$ and $\delta_{\text{B}}(\text{adduct})$ all decrease as Ar^{Cl5} rings are substituted with Ar^{F5} rings. However, compound **9**, while consistent with the general trends, is clearly an outlier for $-E^\circ$ and $\delta_{\text{B}}(\text{borane})$ in which cases its higher and lower (respectively) than the trends would otherwise imply.

The two most prominent outliers, in both cases where $-E^\circ$ is higher than the trends otherwise imply, **5** & **9** (circled in Fig. 4), incorporate a single Ar^{Cl5} ring with a large ($>70^\circ$) twist-angle, leading to the *ortho*-Cl substituents being located above/below the boron centre. As previously suggested (*vide supra*) this orientation allows for significant through-space donation of electron density into the formally vacant boron $2p_z$ orbital,³⁷ thereby reducing the electrophilicity (increasing $-E^\circ$) of the boron from that predicted otherwise by the trend {the observation of **9** as an outlier in the general trend of $\delta_{\text{B}}(\text{borane})$, could also be rationalised similarly}. It should be noted that **9** does not appear as an outlier in plots of $\delta_{\text{P}}(\text{adduct})$ and $\delta_{\text{B}}(\text{adduct})$ (considering the poor trends of the 4–7 series, **5** cannot be identified as an outlier or not), since the geometry changes at the boron centre and the explicit filling of the boron $2p_z$ orbital, eliminates the possibility for electronic effects due to *ortho*-substituents. Similar interactions, leading to the “Gutmann–Beckett method” failing to give adequate measures of Lewis acidity, have been previously noted for ferrocenyl substituted silicon cations; where the cationic silicon interacts with the ferrocenyl backbone, an interaction that is quenched upon adduct formation.⁴³

Considering the correlations between all six combinations of the four measurements (see Fig. S5† for correlation plots), for the entire data set (**1**–**9**), there is little evidence of correlation between any of the potential measures of Lewis acidity with themselves nor with the measure of electrophilicity, $-E^\circ$. However, there are generally linear correlations between all six combinations of measures for the $\text{B}(\text{Ar}^{\text{F5}})_x(\text{Ar}^{\text{F6}})_y$, **1**–**4**, series (which it should be noted, are the only compounds which do not incorporate Ar^{Cl5} substituents).

This lack of clear correlation between any pair of measures of Lewis acidity, particularly that of E° (*i.e.* electrophilicity of the boron centre) and $\delta_{\text{P}}(\text{adduct})$ (*i.e.* the “Gutmann–Beckett” acceptor number) (Fig. S5b†), is not surprising given that the “Gutmann–Beckett method” is highly dependent on steric constraints and adduct formation that will not occur for the most sterically bulky Lewis acids, such as **7**, and the 2,4- and 2,5-isomers of **4**;³⁷ whereas, electron transfer is not influenced to any appreciable extent by the sterics surrounding the boron centre in these tri(aryl)boranes, where the pendant conjugated aryl systems ensure electron transfer to even the most crowded boron centres.³⁷ What these correlations do reveal is that the electrochemical measurements clearly and easily identify outliers for the trends, and that where these occur there is an

obvious, but often unconsidered electronic effect due to the twist-angle of the aryl rings affecting either the donation of electron density into the vacant $2p_z$ orbital on boron from *ortho*-substituents on the rings, or π -electron density from the aryl rings or both.

H₂ cleavage by FLPs

The ability of these boranes to act as the Lewis acidic component of an FLP for the cleavage of H₂ was screened, in combination with the Lewis base P(^tBu)₃ in dichloromethane at room temperature, with the reactions monitored by ¹H and ¹¹B NMR spectroscopy (see Fig. S6–S14†).

In addition to the now well studied **1**, under these mild conditions, **2**, **3**, **5**, **6**, **8** & **9**, irreversibly heterolytically cleave H₂ to generate terminal-tri(aryl)borohydrides; as shown by the observation of a 1 : 1 : 1 : 1 quartet in the ¹H NMR spectra and a doublet in the ¹¹B NMR spectra with ¹J_{HB} coupling of 85–95 Hz (Table 4). (H₂ cleavage has also been previously reported for the Lewis acids **8** & **9**, with the Lewis bases tmp & lutidine at elevated temperatures,^{25,44} and as an equilibrium process with thf as the Lewis base.²³) As previously reported,^{21,37} while **4** rapidly cleaves H₂ it does not lead to generation of a terminal-hydride, but instead to the bridging-hydride species [$\mu\text{-H}(\text{4})_2$][−]. Resonances unequivocally associated with [$\mu\text{-H}(\text{4})_2$][−] could not be distinguished in either the ¹H or ¹¹B NMR spectra (despite [(^tBu)₃PH][$\mu\text{-H}(\text{4})_2$] remaining soluble in CD₂Cl₂). Finally, while 7/P(^tBu)₃ and 7/thf FLPs have previously been shown to cleave H₂, albeit at elevated temperatures,^{23,45} under these mild conditions there was no evidence for reaction of H₂ with the FLP 7/P(^tBu)₃ over a period of five days.

Since all our reactions were performed under the same conditions and monitored throughout, it is possible to make qualitative descriptions as to the kinetics and mechanism(s) of H₂ cleavage by these boranes. We observed the reaction with **1** as the Lewis acid reaching completion fastest (*ca.* 5 hours following H₂ addition), with the reaction time increasing in the order, **1** < **2** \approx **9** < **3** < **8** < **5** \approx **6** (*ca.* 23% conversion, after *ca.* 96 hours). Cleavage with **1**–**3** was near quantitative, while the Lewis acids **5**, **6**, **8** & **9** led to a mixture of products by ¹¹B NMR spectroscopy (the by-products giving signals in the range

Table 4 ¹H and ¹¹B NMR spectral data for the terminal hydride products from the FLP cleavage of H₂

	$\delta_{\text{H}}(\text{HBArHal}_x)/$ ppm	$\delta_{\text{B}}(\text{HBArHal}_x)/$ ppm	¹ J _{HB} / Hz
B(C ₆ F ₅) ₃ 1	+3.61	−25.3	93.9
B(C ₆ F ₅) ₂ {3,5-(CF ₃) ₂ C ₆ H ₃ } 2	+3.69	−19.9	86.1
B{3,5-(CF ₃) ₂ C ₆ H ₃ } ₂ (C ₆ F ₅) 3	+3.71	−14.7	86.1
B{3,5-(CF ₃) ₂ C ₆ H ₃ } ₃ 4	No terminal-hydride formation		
B{3,5-(CF ₃) ₂ C ₆ H ₃ } ₂ (C ₆ Cl ₅) 5	+4.22	−10.0	86.0
B(C ₆ Cl ₅) ₂ {3,5-(CF ₃) ₂ C ₆ H ₃ } 6	+4.24	−8.6	88.0
B(C ₆ Cl ₅) ₃ 7	No reaction		
B(C ₆ Cl ₅) ₂ (C ₆ F ₅) 8	+4.11	−14.3	86.1
B(C ₆ F ₅) ₂ (C ₆ Cl ₅) 9	+3.94	−19.6	90.0

All values herein have been re-measured by the authors.



Table 5 Crystallographic data for 5 and 6

	B{3,5-(CF ₃) ₂ C ₆ H ₃ } ₂ (C ₆ Cl ₅) ₅ 5	B(C ₆ Cl ₅) ₂ {3,5-(CF ₃) ₂ C ₆ H ₃ } 6
Empirical formula	C ₂₂ H ₆ BCl ₅ F ₁₂	C ₂₀ H ₃ BCl ₁₀ F ₆
Formula weight	686.33	722.53
Temperature/K	140(1)	140(1)
Crystal system	Monoclinic	Monoclinic
Space group	C2/c	P2 ₁ /n
a/Å	11.5422(8)	8.5532(17)
b/Å	13.1500(8)	9.742(2)
c/Å	16.6630(10)	30.812(8)
α/°	90.0	90.0
β/°	103.799(7)	90.871(18)
γ/°	90.0	90.0
Volume/Å ³	2456.1(3)	2567.1(10)
Z	4	4
ρ _{calc} /mg mm ⁻³	1.856	1.870
μ/mm ⁻¹	0.696	1.142
F(000)	1344.0	1408.0
Crystal size/mm ³	0.1 × 0.05 × 0.05	0.1 × 0.05 × 0.05
Radiation	Mo Kα (λ = 0.71073 Å)	Mo Kα (λ = 0.71073 Å)
2θ range for data collection	6.688 to 52.724°	5.764 to 52.0°
Index ranges	-11 ≤ h ≤ 14, -16 ≤ k ≤ 16, -20 ≤ l ≤ 20	-10 ≤ h ≤ 9, -12 ≤ k ≤ 12, -38 ≤ l ≤ 36
Reflections collected	9849	20 074
Independent reflections	2506 [R _{int} = 0.0534, R _{sigma} = 0.0572]	5027 [R _{int} = 0.2721, R _{sigma} = 0.3383]
Data/restraints/parameters	2506/0/183	5027/75/357
Goodness-of-fit on F ²	1.009	1.013
Final R indexes [I ≥ 2σ(I)]	R ₁ = 0.0417, wR ₂ = 0.0808	R ₁ = 0.0891, wR ₂ = 0.1457
Final R indexes [all data]	R ₁ = 0.0755, wR ₂ = 0.0925	R ₁ = 0.2819, wR ₂ = 0.2313
Largest diff. peak/hole/e Å ⁻³	0.38/-0.27	0.54/-0.69

δ_B +6 to -3 ppm, corresponding to four-coordinate boron centres – we speculate that some of these could be due to trace moisture and the products of its reaction with the FLP). One feature of note in the ¹H NMR spectra recorded for 1–3 is initially the borohydride resonances are observed as sharp signals before broadening (for 1 and 2, without changing δ_H ; for 3, initially observed at ca. +3.3 ppm and gradually shifting to ca. +3.7 ppm before the signal broadens) to eventually resolve into the characteristic broad 1 : 1 : 1 : 1 quartet. Further, the dissolved H₂ is not observed until the signal has stopped shifting (while it is clearly observed as the reaction progresses for 5, 6, 8 & 9). These observations may provide further clues as to the mechanism of FLP H₂ cleavage, and we intend to investigate them further in later work.

The reactivity of these boranes towards heterolytic H₂ cleavage unsurprisingly depends on both the Lewis acidity and electrophilicity of the boron centre and the steric bulk of the substituents; hence the lack of reactivity under these conditions of the bulky 7 despite its apparently favourable electrophilicity. However, as we have discovered herein, the correlation between the various aryl substituents and the

Lewis acidity – and even the steric buttressing around the boron centre – is by no means simple. There are subtle steric and electronic influences at work (e.g. through space interactions of *ortho*-substituents with the vacant 2p_z orbital affecting both steric orientation of these rings and the electronics of the borane) that this report has highlighted, that require careful consideration when designing potential new Lewis acidic boranes for FLP reactions.

Conclusions

We have synthesised four new hetero-tri(aryl)boranes, 2, 3, 5 & 6. Which, together with three known homo-tri(aryl)boranes, 1, 4 & 7 and two known hetero-tri(aryl)boranes, 8 & 9, give a series of nine compounds linked by stepwise substitution of their aryl rings. Their redox chemistry has been investigated electrochemically, along with their suitability as Lewis acid components of FLP systems for the heterolytic cleavage of H₂ under mild conditions.

Rapid electrochemical techniques and analysis of the *position* and *shape* of the resulting voltammograms allow for the electrophilicity to be quantified along with a qualitative description of the steric shielding around the boron centre. While the correlations both between different spectroscopic measures of Lewis acidity, and between measures of Lewis acidity and electrochemical measures of electrophilicity are generally poor, the electrochemical measurements easily allow us to identify outliers from trends within specific series of substituted boranes. These arise due to electronic effects (such as, interactions of *ortho*-substituents and aryl π orbitals, with the formally vacant boron 2p_z orbital) are not always obvious from spectroscopic measurements of Lewis acidity. Where these electronic interactions are identified, we have found them to correspond to a higher than average twist-angle between the boron trigonal-plane. Whilst steric buttressing and inductive/mesomeric through-bond effects are often considered in the design of new boranes for FLP studies, the degree of twist angle of each aryl ring and the resulting potential for through-space electronic effects is shown to be an important but often unconsidered factor in determining the Lewis acidity and reactivity of these compounds.

While all but one of these compounds cleaves H₂ under mild conditions as part of an FLP, the rate of cleavage depends on both the Lewis acidity/electrophilicity of the boron centre and its surrounding steric bulk. Establishing that while increasing the formal Lewis acidity should increase the rate of reaction, it must be balanced by preventing too much steric bulk around the active site that might inhibit the rate of reaction. However, while these new boranes do not appear to cleave H₂ as rapidly as the archetype 1, these slower reactions afford the opportunity to observe signals arising from potential intermediates formed during H₂ cleavage by NMR spectroscopy. A comprehensive kinetic investigation of these reactions as part of our future work could possibly lead to a



greater understanding of the mechanism of H₂ cleavage by FLPs.

Experimental

All reactions and manipulations were performed under an atmosphere of dry oxygen-free N₂, using either standard Schlenk techniques or in an MBraun UNilab glovebox. All solvents were dried prior to use by refluxing over an appropriate drying agent {Na/benzophenone for *n*-pentane, *n*-hexane, petroleum ether (b.p 40–60 °C) and diethyl ether; Na for toluene; CaH₂ for dichloromethane}, collected by distillation under a dry oxygen-free N₂ atmosphere and stored over 4 Å molecular sieves prior to use.

NMR Spectra were obtained on a Bruker Avance DPX-500 spectrometer; for ¹H spectra residual *protio*-solvent was used as an internal standard; for ¹³C the solvent resonance(s) were used as an internal standard;⁴⁶ for ¹⁹F spectra CFCl₃ was used as an external standard; for ¹¹B spectra BF₃·Et₂O was used as an external standard; for ³¹P spectra 85% H₃PO₄ was used as an external standard.

High resolution mass spectrometry was performed by the EPSRC Mass Spectrometry Service at the University of Swansea. Elemental analyses were performed by the Elemental Analysis Service at London Metropolitan University.

Single crystals of **5** were grown by slow diffusion of a saturated CH₂Cl₂ solution into *n*-hexane at –25 °C, single crystals of **6** were grown from a saturated *n*-hexane solution at –25 °C. For **5** and **6**, suitable crystals were selected, encapsulated in a viscous perfluoropolyether and mounted on an Agilent Technologies Xcaliber-3 single crystal X-ray diffractometer using Mo K α radiation where the crystals were cooled to 140 K during data collection and a full sphere of data collected. The data was reduced and an absorption correction performed using Agilent Technologies CrysAlisPro version 171.37.35.⁴⁷ Using Olex2,⁴⁸ the structures were solved and space group assigned with SuperFlip/EDMA using charge flipping,⁴⁹ and then refined with the ShelXL version 2014/7 refinement program using least squares minimisation.⁵⁰

CCDC 1418145 (**5**), and 1418144 (**6**) contains the supplementary crystallographic data for this paper.

Electrochemical studies were carried out using a Metrohm Autolab μ -II, PGSTAT30 or PGSTAT302N potentiostat linked to a computer running Metrohm Autolab NOVA version 1.11 software, in conjunction with a three electrode cell comprising: a glassy carbon disc working electrode (Bioanalytical Systems, Inc., ca. 7.0 mm² area calibrated using the [FeCp₂]^{0/+} redox couple), a platinum wire (99.99% purity) counter electrode, and a silver wire (99.99% purity) *pseudo*-reference electrode. All working electrodes were polished with 0.3 μ m α -alumina and dried prior to use. All electrochemical measurements were performed at ambient temperature under a dry N₂ atmosphere (using either a custom-built electrochemical cell or within a glovebox), in CH₂Cl₂ containing 50 mM [ⁿBu₄N][B(C₆F₅)₄] as the supporting electrolyte and between 1.5 and 2.5 mM of the

analyte species of interest. Cyclic voltammetric measurements were, where possible, iR-compensated using positive-feedback to within 85 \pm 5% of the uncompensated solution resistance (ca. 666 Ω). [ⁿBu₄N][B(C₆F₅)₄] was synthesised according to published methods.⁵¹ All potentials were referenced to the [FeCp₂]^{0/+} redox couple, which was added as an internal standard. Simulations of electrochemical processes were performed using ElchSoft DigiElch version 7.096 software.⁵²

B{3,5-(CF₃)₂C₆H₃}₂Br,³⁸ Cu(C₆F₅)₂,⁵³ Zn(C₆Cl₅)₂, B(C₆Cl₅)₃,⁷ and B(C₆F₅)₂(C₆Cl₅)⁹,²⁴ were synthesised as previously reported. Characterisation data for the intermediate B{3,5-(CF₃)₂C₆H₃}₂(OMe)₂, and the impurity B{3,5-(CF₃)₂C₆H₃}₂(OH) is detailed in the ESI.† All other reagents were obtained from commercial suppliers and used as supplied.

B{3,5-(CF₃)₂C₆H₃}₂Br₂

ⁿBuLi (6.25 cm³, 10 mmol, 1.6 M in hexanes) was slowly added to a cooled (–78 °C) solution of 3,5-bis(trifluoromethyl)bromobenzene (1.72 cm³, 10 mmol) in Et₂O (20 cm³) and stirred for 10 min. BH₃·SMe₂ (0.95 cm³, 10 mmol) is added, and after 10 min the reaction mixture warmed to room temperature and stirred for a further 30 min. Me₃SiCl (1.27 cm³, 10 mmol) is added to the clear orange solution, resulting in the rapid formation of a white precipitate, the mixture is stirred for 30 min. Methanol (1.2 cm³, 30 mmol) is slowly added, resulting in rapid evolution of H₂, and the mixture stirred for an hour. Volatiles are removed *in vacuo* to give a cloudy white oil; the intermediate B{3,5-(CF₃)₂C₆H₃}₂(OMe)₂ is extracted into 25 cm³ petroleum ether and isolated as a clear pale yellow solution by filtration (*via cannula*). BBr₃ (2.0 cm³, 20.8 mmol) is added and the mixture stirred for 30 min, the mixture is once again filtered (*via cannula*) isolating a clear pale yellow solution, all volatiles are removed *in vacuo* to give the product as a highly reactive yellow oil. Yield 1.63 g (4.2 mmol, 42%).

¹H NMR (500.21 MHz, CD₂Cl₂, 25 °C, δ): +8.66 (s, 2H, Ar^{F6} 2,6-H), +8.20 (s, 1H, Ar^{F6} 4-H); ¹¹B NMR (160.49 MHz, CD₂Cl₂, 25 °C, δ): +57.3 (br.s); ¹⁹F NMR (470.67 MHz, CD₂Cl₂, 25 °C, δ): –63.3 (s, 6F, Ar^{F6} 3,5-CF₃).

B(C₆F₅)₂{3,5-(CF₃)₂C₆H₃}₂

Solutions of freshly prepared B{3,5-(CF₃)₂C₆H₃}₂Br₂ (1.62 g, 4.2 mmol) in 10 cm³ CH₂Cl₂ and Cu(C₆F₅)₂ (2.30 g, 10 mmol) in 40 cm³ CH₂Cl₂ are combined, and stirred for ca. 1 hour. The reaction mixture is filtered (*via cannula*) to remove the blue-grey precipitate, isolating the clear pale yellow solution, volatiles are removed *in vacuo* to give the off-white solid product. Yield: 1.78 g (3.2 mmol, 77%). The product can be further purified by sublimation at 10^{–1} mbar / 90 °C.

¹H NMR (500.21 MHz, CD₂Cl₂, 25 °C, δ): +8.22 (s, 1H, Ar^{F6} 4-H), +8.15 (s, 2H, Ar^{F6} 2,6-H); ¹¹B NMR (160.49 MHz, CD₂Cl₂, 25 °C, δ): +63.5 (br.s); ¹³C{¹H} NMR (125.78 MHz, CD₂Cl₂, 25 °C, δ): +148.3 (br.d, ¹J_{CF} = 248 Hz, Ar^{F5} 2,6-C), +145.2 (br.d, ¹J_{CF} = 260 Hz, Ar^{F5} 4-C), +141.3 (br.s, Ar^{F6} 1-C), +138.4 (br.d, ¹J_{CF} = 255 Hz, Ar^{F5} 3,5-C), +137.6 (br.q, ³J_{CF} = 1.8 Hz, Ar^{F6} 2,6-C), +132.2 (q, ²J_{CF} = 33.5 Hz, Ar^{F6} 3,5-C), +128.9 (sept., ³J_{CF} = 3.7 Hz, Ar^{F6} 4-C), +123.7 (q, ¹J_{CF} = 273 Hz, Ar^{F6} 3,5-CF₃);



^{19}F NMR (470.67 MHz, CD_2Cl_2 , 25 °C, δ): -63.3 (s, 6F, Ar^{F6} 3,5-CF₃), -127.3 (m, 4F, Ar^{F5} 2,6-F), -145.2 (t, $^3J_{\text{FF}} = 18.7$ Hz, 2F, Ar^{F5} 4-F), -160.4 (m, 4F, Ar^{F5} 3,5-F). HRMS-APCI (m/z): $[\text{M}]^+$ calc. for $\text{C}_{20}\text{H}_3\text{BF}_{16}$, 558.0070; found, 558.0063. Elemental analysis (calc. for $\text{C}_{20}\text{H}_3\text{BF}_{16}$): C 43.17 (43.03), H 0.57 (0.54).

$\text{B}\{3,5\text{-(CF}_3)_2\text{C}_6\text{H}_3\}_2(\text{C}_6\text{F}_5)_3$ 3

Solutions of $\text{B}\{3,5\text{-(CF}_3)_2\text{C}_6\text{H}_3\}_2\text{Br}$ (0.72 g, 1.0 mmol) in 10 cm^3 CH_2Cl_2 and $\text{Cu}(\text{C}_6\text{F}_5)$ (0.23 g, 1.0 mmol) in 10 cm^3 CH_2Cl_2 are combined, and stirred for *ca.* 1 hour. The reaction mixture is filtered (*via* cannula) to remove the precipitate, isolating the clear pale yellow solution, volatiles are removed *in vacuo* to give the off-white solid product. Yield: 0.46 g (0.75 mmol, 75%). The product can be further purified by sublimation at 10^{-1} mbar / 110 °C.

^1H NMR (500.21 MHz, CD_2Cl_2 , 25 °C, δ): +8.22 (s, 2H, Ar^{F6} 4-H), +8.07 (s, 4H, Ar^{F6} 2,6-H); ^{11}B NMR (160.49 MHz, CD_2Cl_2 , 25 °C, δ): +66.0 (br.s); $^{13}\text{C}\{^1\text{H}\}$ NMR (125.78 MHz, CD_2Cl_2 , 25 °C, δ): +148.3 (br.d, $^1J_{\text{CF}} = 250$ Hz, Ar^{F5} 2,6-C), +144.9 (br.d, $^1J_{\text{CF}} = 260$ Hz, Ar^{F5} 4-C), +142.3 (br.s, Ar^{F6} 1-C), +138.5 (br.d, $^1J_{\text{CF}} = 255$ Hz, Ar^{F5} 3,5-C), +137.7 (br.q, $^3J_{\text{CF}} = 2.3$ Hz, Ar^{F6} 2,6-C), +132.3 (q, $^2J_{\text{CF}} = 33.0$ Hz, Ar^{F6} 3,5-C), +127.9 (sept., $^3J_{\text{CF}} = 3.7$ Hz, Ar^{F6} 4-C), +123.8 (q, $^1J_{\text{CF}} = 273$ Hz, Ar^{F6} 3,5-CF₃), +113.2 (br.s, Ar^{F5} 1-C); ^{19}F NMR (470.67 MHz, CD_2Cl_2 , 25 °C, δ): -63.4 (s, 12F, Ar^{F6} 3,5-CF₃), -126.0 (m, 2F, Ar^{F5} 2,6-F), -146.0 (tt, $^3J_{\text{FF}} = 19.9$ Hz, $^4J_{\text{FF}} = 4.2$ Hz, 1F, Ar^{F5} 4-F), -160.1 (m, 2F, Ar^{F5} 3,5-F). HRMS-APCI (m/z): $[\text{M} - \text{H}]^+$ calc. for $\text{C}_{22}\text{H}_5\text{BF}_{17}$, 603.0211; found, 603.0201. Elemental analysis (calc. for $\text{C}_{22}\text{H}_5\text{BF}_{17}$): C 43.86 (43.73), H 1.08 (1.00).

$\text{B}(\text{C}_6\text{Cl}_5)_2\text{Cl}$

C_6Cl_6 (14.24 g, 50 mmol) was suspended in Et_2O (≥ 300 cm^3) and the slurry cooled to -78 °C. $^n\text{BuLi}$ (35.5 cm^3 , 50 mmol, 1.41 M in hexanes) was added, and the cooled reaction mixture stirred for 4 hours to give a clear golden solution. Cooled (-78 °C) *n*-pentane (≥ 300 cm^3) was added to give a fine white precipitate of LiC_6Cl_5 ; after 30 min, BCl_3 (25 cm^3 , 25 mmol, 1.0 M in heptane) was slowly added, and the reaction mixture slowly warmed to room temperature and stirred for 12 hours. Removal of volatiles *in vacuo*, gave a pale orange solid; the product was extracted with toluene (3×100 cm^3) and isolated by filtration to give an amber solution. Removal of volatiles *in vacuo*, washing with *n*-hexane, and drying *in vacuo*, gave $\text{B}(\text{C}_6\text{Cl}_5)_2\text{Cl}$ as a pale yellow solid. Yield: 8.80 g (16.1 mmol, 64.4%).

Characterisation data as previously reported in ref. 24.

$\text{B}\{3,5\text{-(CF}_3)_2\text{C}_6\text{H}_3\}_2(\text{C}_6\text{Cl}_5)_3$ 5

$\text{B}\{3,5\text{-(CF}_3)_2\text{C}_6\text{H}_3\}_2\text{Br}$ (1.00 g, 1.93 mmol) and $\text{Zn}(\text{C}_6\text{Cl}_5)_2$ (0.55 g, 0.97 mmol) are combined and suspended in 10 cm^3 toluene. The reaction vessel is sealed and heated at *ca.* 75 °C for *ca.* 72 hours. Once cooled volatiles are removed *in vacuo*, and the product extracted into CH_2Cl_2 giving a pale green solution. The solid is precipitated by, addition of *n*-hexane, concentration *in vacuo*, and cooling at -25 °C. The micro-crystalline

pale green solid was isolated and dried *in vacuo*. Yield: 0.46 g (0.64 mmol, 33%).

^1H NMR (500.21 MHz, CD_2Cl_2 , 25 °C, δ): +8.20 (s, 2H, Ar^{F6} 4-H), +8.13 (s, 4H, Ar^{F6} 2,6-H); ^{11}B NMR (160.49 MHz, CD_2Cl_2 , 25 °C, δ): +65.7 (br.s); $^{13}\text{C}\{^1\text{H}\}$ NMR (125.78 MHz, CD_2Cl_2 , 25 °C, δ): +137.4 (br.q, $^3J_{\text{CF}} = 3.7$ Hz, Ar^{F6} 2,6-C) +135.4 (s, Ar^{Cl5} 4-C), +132.9 (s, Ar^{Cl5} 2,6/3,5-C), +132.3 (q, $^2J_{\text{CF}} = 33.0$ Hz, Ar^{F6} 3,5-C), +131.4 (s, Ar^{Cl5} 2,6/3,5-C), +127.7 (sept., $^3J_{\text{CF}} = 3.7$ Hz, Ar^{F6} 4-C), +123.6 (q, $^1J_{\text{CF}} = 273$ Hz, Ar^{F6} 3,5-CF₃); ^{19}F NMR (470.67 MHz, CD_2Cl_2 , 25 °C, δ): -63.2 (s, 12F, Ar^{F6} 3,5-CF₃). HRMS-APCI (m/z): $[\text{M}]^+$ calc. for $\text{C}_{22}\text{H}_6\text{BCl}_5\text{F}_{12}$, 685.8784; found, 685.8773. Elemental analysis (calc. for $\text{C}_{22}\text{H}_6\text{BCl}_5\text{F}_{12}$): C 38.62 (38.49), H 0.81 (0.88).

$\text{B}(\text{C}_6\text{Cl}_5)_2\{3,5\text{-(CF}_3)_2\text{C}_6\text{H}_3\}_6$ 6

$^n\text{BuLi}$ (1.56 cm^3 , 2.2 mmol, 1.41 M in hexanes) was slowly added to a cooled (-78 °C) solution of 3,5-bis(trifluoromethyl)-bromobenzene (0.38 cm^3 , 2.2 mmol) in Et_2O (50 cm^3) and left to stir for 1 hour. $\text{B}(\text{C}_6\text{Cl}_5)_2\text{Cl}$ (1.23 g, 2.3 mmol) was dissolved in toluene (20 cm^3), cooled (-78 °C), and slowly added to the reaction mixture, which was left to stir at -78 °C for 3 hours and then slowly warmed to room temperature over 18 hours. Removal of volatiles *in vacuo*, gave a pale yellow solid. This was extracted with *n*-hexane (2×50 cm^3), which after removal of volatiles *in vacuo*, gave a light yellow powder. Yield 0.78 g (1.1 mmol, 50%).

^1H NMR (500.21 MHz, CD_2Cl_2 , 25 °C, δ): +8.15 (s, 1H, Ar^{F6} 4-H), +8.03 (s, 2H, Ar^{F6} 2,6-H); ^{11}B NMR (160.49 MHz, CD_2Cl_2 , 25 °C, δ): +66.0 (br.s); $^{13}\text{C}\{^1\text{H}\}$ NMR (125.78 MHz, CD_2Cl_2 , 25 °C, δ): +137.3 (br.q, $^3J_{\text{CF}} = 2.3$ Hz, Ar^{F6} 2,6-C) +137.0 (s, Ar^{Cl5} 4-C), +133.5 (s, Ar^{Cl5} 2,3,5,6-C), +132.5 (q, $^2J_{\text{CF}} = 33.4$ Hz, Ar^{F6} 3,5-C), +128.4 (sept., $^3J_{\text{CF}} = 3.8$ Hz, Ar^{F6} 4-C), +123.7 (q, $^1J_{\text{CF}} = 273$ Hz, Ar^{F6} 3,5-CF₃); ^{19}F NMR (470.67 MHz, CD_2Cl_2 , 25 °C, δ): -63.3 (s, 6F, Ar^{F6} 3,5-CF₃). HRMS-APCI (m/z): $[\text{M}]^+$ calc. for $\text{C}_{20}\text{H}_3\text{BCl}_{10}\text{F}_6$, 721.7058; found, 721.7054. Elemental analysis (calc. for $\text{C}_{20}\text{H}_3\text{BCl}_{10}\text{F}_6$): C 33.36 (33.24), H 0.50 (0.42).

$\text{B}(\text{C}_6\text{Cl}_5)_2(\text{C}_6\text{F}_5)_3$ 8

$^n\text{BuLi}$ (1.40 cm^3 , 1.97 mmol, 1.41 M in hexanes) was slowly added to a cooled (-78 °C) solution of bromopentafluorobenzene (0.25 cm^3 , 2.0 mmol) in toluene (50 cm^3) and stirred for 15 minutes. A solution of $\text{B}(\text{C}_6\text{Cl}_5)_2\text{Cl}$ (1.09 g, 2.0 mmol) in toluene (20 cm^3) was then slowly added to the reaction mixture, which was subsequently left to warm to room temperature over 18 hours. The solution was filtered through celite (*via* cannula), and the volatiles removed *in vacuo* to give a sticky amber solid. This was then extracted with *n*-pentane (5 cm^3), which when cooled (-78 °C) precipitated the product as a pale yellow powder. Yield: 0.28 g (0.41 mmol, 21%).

Characterisation data as previously reported in ref. 24.

Acknowledgements

G. G. W. thanks the Royal Society for financial support by a University Research Fellowship. The research leading to these



results has received funding from the European Research Council under the ERC Grant Agreements no. 307061 (PiHOMER) and 640988 (FLPower). We acknowledge the use of the EPSRC funded National Chemical Database Service hosted by the Royal Society of Chemistry, and the EPSRC UK National Mass Spectrometry Facility (NMSF) at the University of Swansea. We thank the Research Computing Service at the University of East Anglia for access to the high performance computing cluster.

References

- G. C. Welch and D. W. Stephan, *J. Am. Chem. Soc.*, 2007, **129**, 1880–1881.
- D. W. Stephan, *Dalton Trans.*, 2009, 3129–3136.
- D. W. Stephan and G. Erker, *Angew. Chem., Int. Ed.*, 2010, **49**, 46–76.
- D. W. Stephan, *Comp. Inorg. Chem. II*, 2013, **1**, 1069–1103.
- D. W. Stephan and G. Erker, *Chem. Sci.*, 2014, **5**, 2625–2641.
- D. W. Stephan and G. Erker, *Angew. Chem., Int. Ed.*, 2015, **54**, 6400–6441.
- D. W. Stephan, *J. Am. Chem. Soc.*, 2015, **137**, 10018–10032.
- T. Mahdi and D. W. Stephan, *J. Am. Chem. Soc.*, 2012, **136**, 15809–15812.
- Á. Gyömöre, M. Bakos, T. Földes, I. Pápai, A. Domján and T. Soós, *ACS Catal.*, 2015, **5**, 5366–5372.
- D. J. Scott, M. J. Fuchter and A. E. Ashley, *J. Am. Chem. Soc.*, 2014, **136**, 15813–15816; D. J. Scott, T. R. Simmons, E. J. Lawrence, G. G. Wildgoose, M. J. Fuchter and A. E. Ashley, *ACS Catal.*, 2015, **5**, 5540–5544.
- T. Mahdi, J. N. del Castillo and D. W. Stephan, *Organometallics*, 2013, **32**, 1971–1978.
- P. A. Chase, G. C. Welch, T. Jurca and D. W. Stephan, *Angew. Chem., Int. Ed.*, 2007, **46**, 8050–8053.
- H. Wang, R. Fröhlich, G. Kehra and G. Erker, *Chem. Commun.*, 2008, 5966–5968.
- G. Ménard, T. M. Gilbert, J. A. Hatnean, A. Kraft, I. Krossing and D. W. Stephan, *Organometallics*, 2013, **32**, 4416–4422.
- Z. Lu, Y. Wang, J. Liu, Y. jian Lin, Z. H. Li and H. Wang, *Organometallics*, 2013, **32**, 6753–6758.
- A. E. Ashley, A. L. Thompson and D. O'Hare, *Angew. Chem., Int. Ed.*, 2009, **48**, 9839–9843.
- E. Otten, R. C. Neu and D. W. Stephan, *J. Am. Chem. Soc.*, 2009, **131**, 9918–9919.
- M. Sajid, A. Klose, B. Birkmann, L. Liang, B. Schirmer, T. Wiegand, H. Eckert, A. J. Lough, R. Fröhlich, C. G. Daniliuc, S. Grimme, D. W. Stephan, G. Kehr and G. Erker, *Chem. Sci.*, 2013, **4**, 213–219.
- J. S. J. McCahill, G. C. Welch and D. W. Stephan, *Angew. Chem., Int. Ed.*, 2007, **46**, 4968–4971.
- M. A. Dureen and D. W. Stephan, *J. Am. Chem. Soc.*, 2009, **131**, 8396–8397.
- T. J. Herrington, A. J. W. Thom, A. J. P. White and A. E. Ashley, *Dalton Trans.*, 2012, **41**, 9019–9022.
- S. C. Binding, H. Zaher, F. M. Chadwick and D. O'Hare, *Dalton Trans.*, 2012, **41**, 9061–9066.
- D. J. Scott, M. J. Fuchter and A. E. Ashley, *Angew. Chem., Int. Ed.*, 2014, **53**, 10218–10222.
- A. E. Ashley, T. J. Herrington, G. G. Wildgoose, H. Zaher, A. L. Thompson, N. H. Rees, T. Krämer and D. O'Hare, *J. Am. Chem. Soc.*, 2011, **133**, 14727–14740.
- D. O'Hare and A. Ashley, *US Pat*, 2012/0283340A1, 2012.
- S. A. Cummings, M. Iimura, C. J. Harlan, R. J. Kwaan, I. V. Trieu, J. R. Norton, B. M. Bridgewater, F. Jäkle, A. Sundararaman and M. Tilset, *Organometallics*, 2006, **25**, 1565–1568.
- J. M. Farrell, J. A. Hatnean and D. W. Stephan, *J. Am. Chem. Soc.*, 2012, **134**, 15728–15731.
- E. J. Lawrence, T. J. Herrington, A. E. Ashley and G. G. Wildgoose, *Angew. Chem., Int. Ed.*, 2014, **53**, 9922–9925.
- E. R. Clark and M. J. Ingleson, *Angew. Chem., Int. Ed.*, 2014, **53**, 11306–11309.
- G. Ménard and D. W. Stephan, *Angew. Chem., Int. Ed.*, 2012, **53**, 8272–8275.
- J. M. Bayne and D. W. Stephan, *Chem. Soc. Rev.*, 2015, DOI: 10.1039/c5cs00516g.
- A. Schäfer, M. Reißmann, A. Schäfer, W. Saak, D. Haase and T. Müller, *Angew. Chem., Int. Ed.*, 2011, **50**, 12636–12638.
- B. Waerder, M. Pieper, L. A. Körte, T. A. Kinder, A. Mix, B. Neumann, H.-G. Stammer and N. W. Mitzel, *Angew. Chem., Int. Ed.*, 2015, DOI: 10.1002/anie.201504171.
- E. J. Lawrence, V. S. Oganessian, G. G. Wildgoose and A. E. Ashley, *Dalton Trans.*, 2013, **42**, 782–789.
- E. J. Lawrence, V. S. Oganessian, D. L. Hughes, A. E. Ashley and G. G. Wildgoose, *J. Am. Chem. Soc.*, 2014, **136**, 6031–6036.
- E. J. Lawrence, R. J. Blagg, D. L. Hughes, A. E. Ashley and G. G. Wildgoose, *Chem. – Eur. J.*, 2015, **21**, 900–906.
- R. J. Blagg, E. J. Lawrence, K. Resner, V. S. Oganessian, T. J. Herrington, A. E. Ashley and G. G. Wildgoose, *Dalton Trans.*, 2015, DOI: 10.1039/c5dt01918d.
- K. Samigullin, M. Bolte, H.-W. Lerner and M. Wagner, *Organometallics*, 2014, **33**, 3564–3569.
- W. V. Konze, B. L. Scott and G. J. Kubas, *Chem. Commun.*, 1999, 1807–1808.
- U. Mayer, V. Gutmann and W. Gerger, *Monatsh. Chem.*, 1975, **106**, 1235–1257.
- M. A. Beckett, G. C. Strickland, J. R. Holland and K. S. Varma, *Polymer*, 1996, **37**, 4629–4631.
- I. B. Sivaev and V. I. Bregadze, *Coord. Chem. Rev.*, 2014, **270–271**, 75–88.
- A. R. Nödling, K. Mütter, V. H. G. Rohde, G. Hilt and M. Oestreich, *Organometallics*, 2014, **33**, 302–308.
- H. Zaher, A. E. Ashley, M. Irwin, A. L. Thompson, M. J. Gutmann, T. Krämera and D. O'Hare, *Chem. Commun.*, 2013, **49**, 9755–9757.



- 45 A. L. Travis, S. C. Binding, H. Zaher, T. A. Q. Arnold, J.-C. Buffet and D. O'Hare, *Dalton Trans.*, 2013, **42**, 2431–2437.
- 46 G. R. Fulmer, A. J. M. Miller, N. H. Sherden, H. E. Gottlieb, A. Nudelman, B. M. Stoltz, J. E. Bercaw and K. I. Goldberg, *Organometallics*, 2010, **29**, 2176–2179.
- 47 *CrysAlisPro*, Agilent Technologies, Yarnton, UK.
- 48 L. J. Bourhis, O. V. Dolomanov, R. J. Gildea, J. A. K. Howard and H. Puschmann, *Acta Crystallogr., Sect. A: Fundam. Crystallogr.*, 2015, **71**, 59–75; O. V. Dolomanov, L. J. Bourhis, R. J. Gildea, J. A. K. Howard and H. Puschmann, *J. Appl. Crystallogr.*, 2009, **42**, 339–341.
- 49 L. Palatinus and G. Chapuis, *J. Appl. Crystallogr.*, 2007, **40**, 786–790; L. Palatinus and A. van der Lee, *J. Crystallogr. Cryst.*, 2008, **41**, 975–984; L. Palatinus, S. J. Prathapab and S. van Smaalen, *J. Appl. Crystallogr.*, 2012, **45**, 575–580.
- 50 G. M. Sheldrick, *Acta Crystallogr., Sect. C: Cryst. Struct. Commun.*, 2015, **71**, 3–8; G. M. Sheldrick, *Acta Crystallogr., Sect. A: Fundam. Crystallogr.*, 2008, **64**, 112–122.
- 51 S. Lancaster, *ChemSpider Synthetic Pages*, 2003, DOI: 10.1039/SP215, <http://cssp.chemspider.com/215>; T. E. Krafft, *US Pat*, 5,679,289, Boulder Scientific Company, 1997; R. J. LeSuer, C. Buttolph and W. E. Geiger, *Anal. Chem.*, 2004, **76**, 6395–6401.
- 52 *DigiElch-Professional*, ElechSoft, Kleinromstedt, Germany.
- 53 A. Cairncross, W. A. Sheppard and E. Wonchoba, *Org. Synth.*, 1979, **59**, 122.

